The Astrophysical Journal, 753:174 (10pp), 2012 July 10 doi:10.1088/0004-637X/753/2/174

DISCOVERY OF THE OPTICAL/ULTRAVIOLET/GAMMA-RAY COUNTERPART TO THE ECLIPSING MILLISECOND PULSAR J1816+4510

D. L. Kaplan[1,2], K. Stovall[3,4], S. M. Ransom[5], M. S. E. Roberts[6,7], R. Kotulla[1], A. M. Archibald[8], C. M. Biwer[1], J. Boyles[9], L. Dartez[3], D. F. Day[1], A. J. Ford[3], A. Garcia[3], J. W. T. Hessels[10,11], F. A. Jenet[3], C. Karako[8], V. M. Kaspi[8], V. I. Kondratiev[10,12], D. R. Lorimer[9,14], R. S. Lynch[8], M. A. McLaughlin[9,14], M. D. W. Rohr[1], X. Siemens[1], I. H. Stairs[13], and J. van Leeuwen[10,11]

[1] Physics Department, University of Wisconsin-Milwaukee, Milwaukee WI 53211, USA; kaplan@uwm.edu
[2] Department of Astronomy, University of Wisconsin-Madison, Madison, WI, USA
[3] Center for Advanced Radio Astronomy and Department of Physics and Astronomy, University of Texas at Brownsville, Brownsville, TX 78520, USA
[4] Department of Physics and Astronomy, University of Texas at San Antonio, San Antonio, TX 78249, USA
[5] National Radio Astronomy Observatory, 520 Edgemont Road, Charlottesville, VA 22901, USA
[6] Eureka Scientific, Inc., 2452 Delmer Street, Suite 100, Oakland, CA 94602-3017, USA
[7] Department of Physics, Ithaca College, Ithaca, NY 14850, USA
[8] Department of Physics, McGill University, 3600 University Street, Montreal, QC H3A 2T8, Canada
[9] Department of Physics, West Virginia University, White Hall, 115 Willey Street, Morgantown, WV 26506, USA
[10] ASTRON, the Netherlands Institute for Radio Astronomy, Postbus 2, 7990 AA, Dwingeloo, The Netherlands
[11] Astronomical Institute "Anton Pannekoek," University of Amsterdam, Science Park 904, 1098 XH Amsterdam, The Netherlands
[12] Astro Space Center of the Lebedev Physical Institute, Profsoyuznaya str. 84/32, Moscow 117997, Russia
[13] Department of Physics and Astronomy, University of British Columbia, 6224 Agricultural Road, Vancouver, BC V6T 1Z1, Canada
Received 2012 March 2; accepted 2012 May 8; published 2012 June 26

ABSTRACT

The energetic, eclipsing millisecond pulsar J1816+4510 was recently discovered in a low-frequency radio survey with the Green Bank Telescope. With an orbital period of 8.7 hr and a minimum companion mass of 0.16 $M_\odot$, it appears to belong to an increasingly important class of pulsars that are ablating their low-mass companions. We report the discovery of the γ-ray counterpart to this pulsar and present a likely optical/ultraviolet counterpart as well. Using the radio ephemeris, we detect pulsations in the unclassified γ-ray source 2FGL J1816.5+4511, implying an efficiency of $\sim$25% in converting the pulsar's spin-down luminosity into γ-rays and adding PSR J1816+4510 to the large number of millisecond pulsars detected by *Fermi*. The likely optical/UV counterpart was identified through position coincidence ($<0\farcs1$) and unusual colors. Assuming that it is the companion, with $R = 18.27 \pm 0.03$ mag and effective temperature $\gtrsim$15,000 K, it would be among the brightest and hottest of low-mass pulsar companions and appears qualitatively different from other eclipsing pulsar systems. In particular, current data suggest that it is a factor of two larger than most white dwarfs of its mass but a factor of four smaller than its Roche lobe. We discuss possible reasons for its high temperature and odd size, and suggest that it recently underwent a violent episode of mass loss. Regardless of origin, its brightness and the relative unimportance of irradiation make it an ideal target for a mass, and hence a neutron star mass, determination.

Key words: binaries: eclipsing – gamma rays: stars – pulsars: individual (PSR J1816+4510) – ultraviolet: stars – white dwarfs

Online-only material: color figures

1. INTRODUCTION

The 3.2 ms pulsar J1816+4510 was discovered as part of the Green Bank North Celestial Cap (GBNCC) survey (K. Stovall et al. 2012, in preparation)—a survey of the sky north of declination +38° at 350 MHz with the 100 m Robert C. Byrd Green Bank Telescope—in a pointing selected for being coincident with an unclassified *Fermi* γ-ray source (a successful search strategy, as shown in Hessels et al. 2011; Ransom et al. 2011; Cognard et al. 2011; Keith et al. 2011; Kerr et al. 2012, and others). Shortly after discovery, it was realized that the radio data showed evidence for acceleration in an 8.66 hr circular orbit, with eclipses lasting up to 10% of the orbit at 350 MHz (Figure 1). Eclipsing millisecond pulsars, especially those with γ-ray counterparts, are often associated with "black-widow" or "redback" systems. These systems harbor low-mass companions ($\lesssim$0.05 $M_\odot$ for black-widows and $\sim$0.2 $M_\odot$ for redbacks; Fruchter et al. 1988; D'Amico et al. 2001; Archibald et al. 2009) and have been discovered with increasing frequency in recent years (see Roberts 2011 for a recent review), often in globular clusters. The eclipses are typically long (they can cover most of the orbit; Archibald et al. 2009; Hessels et al. 2011), implying eclipsing regions larger than the Roche lobes of the companions, and there are regions of the orbit where the pulsar is seen through ionized plasma that delays the pulses compared to the expected ephemeris. The basic model for these sources is one in which the energetic wind from the pulsar irradiates and ablates the companion, leading to long eclipses from ionized material in the systems (e.g., Stappers et al. 2001). The companions are usually tidally distorted, filling a significant fraction of their Roche lobes (Reynolds et al. 2007), which, along with heating from the pulsar's wind, leads to significant (often >3 mag at wavelengths of around 5000 Å) optical modulation. Such systems are interesting both because they provide a probe of the interaction between the pulsar's wind and the companion and,

[14] Also adjunct at the National Radio Astronomy Observatory, Green Bank, WV 24944M, USA.

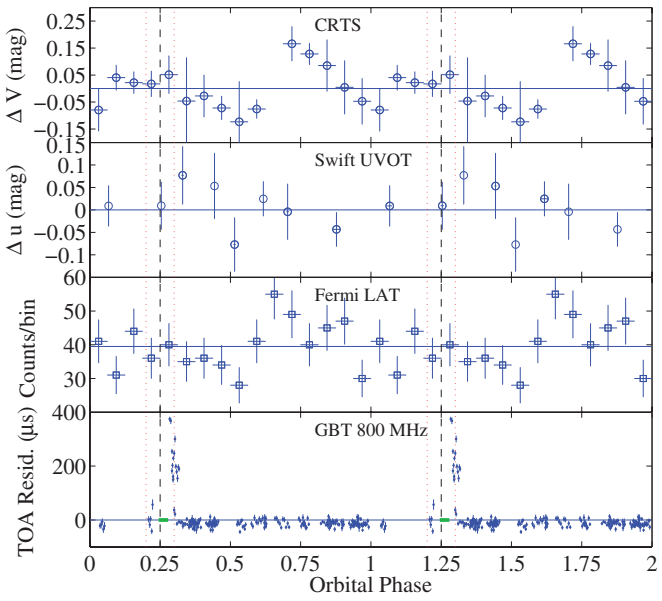

Figure 1. Orbital behavior of the radio times of arrival (residuals at 820 MHz in μs from K. Stovall et al. 2012, in preparation; bottom), *Fermi* LAT 0.3–10 GeV count rate (second from bottom), *Swift* UVOT *u*-band photometry (relative to the mean; second from top), and CRTS *V*-band photometry (relative to the mean; top) vs. orbital phase, repeated twice for clarity. The horizontal lines are for reference at the mean magnitude, count rate, and at 0 residual. The *Swift* data have a scatter consistent with the uncertainties, with $\chi^2 = 5.4$ for 7 degrees of freedom relative to a constant model. For the *Fermi* data, $\chi^2 = 20.9$ for 15 degrees of freedom. The CRTS data may show some orbital modulation ($\chi^2 = 29.2$ for 14 degrees of freedom) that shares some of the shape of the *Fermi* data, but that needs to be confirmed. The vertical dashed lines are the times of conjunction (eclipse), while the vertical dotted lines show the approximate observed limits on the eclipse duration. In the radio panel, the thick green segments show the phase region where we have observations but the source was not detected.

(A color version of this figure is available in the online journal.)

ultimately, because such systems allow measurement of neutron star masses through binary modeling (van Kerkwijk et al. 2011).

Here, we report on new and archival optical and ultraviolet data on the counterpart of PSR J1816+4510. We use these data, along with archival γ-ray data from the *Fermi* spacecraft, to constrain the nature of the PSR J1816+4510 system. The outline of this paper is as follows: we first describe the archival optical and ultraviolet data that we used to identify the counterpart to PSR J1816+4510 (Section 2.1), and then we discuss new optical data from the Wisconsin Indiana Yale NOAO telescope (Section 2.2). We fit the optical/ultraviolet spectral energy distribution (SED) in Section 2.3. We then discuss the *Fermi* γ-ray data (Section 3.2) and the *Swift* X-ray upper limits (Section 3.1). Finally, we discuss the implications of our data in Section 4, and conclude in Section 5.

1.1. System Parameters

We make use of the radio ephemeris for PSR J1816+4510 determined by K. Stovall et al. (2012, in preparation): position $\alpha = 18^{\rm h}16^{\rm m}35\overset{\rm s}{.}9314(2) \delta = +45^\circ10'33\overset{''}{.}864(2)$ (J2000), binary period $P_b = 8.66$ hr, and minimum companion mass $M_c = 0.162\,M_\odot$ (assuming a neutron star mass of $1.4\,M_\odot$, although a somewhat more massive neutron star may be likely given likely accretion histories; Verbiest et al. 2008; van Kerkwijk et al. 2011). Such a companion mass would put it among the "redback" class (Roberts 2011), although if the companion is more degenerate it might instead contain a He-core white dwarf such as that in the PSR J1911−5958A system (Bassa et al. 2006). If the orbit is edge-on, then the full semimajor axis is $a = 2.46\,R_\odot$ with a Roche lobe radius $R_L = 0.53\,R_\odot$ (based on Eggleton 1983). The dispersion-measure (DM) distance is 2.4 kpc (Cordes & Lazio 2002, for a DM of 38.8 cm^{-3} pc), although given the high Galactic latitude ($b = 24\overset{\circ}{.}7$), the uncertainties are large and this could be an underestimate (Gaensler et al. 2008; Chatterjee et al. 2009; Roberts 2011). Therefore, we approximate the distance as 2 kpc and parameterize it as $d = 2d_2$ kpc, with a nominal value of $d_2 = 1.2$. In what follows, other fundamental parameters for PSR J1816+4510 that are not explicitly cited are based on K. Stovall et al. (2012, in preparation).

2. OPTICAL AND ULTRAVIOLET DATA AND ANALYSIS

2.1. Archival Optical/UV Data

We initially identified a potential counterpart to PSR J1816+4510 in the USNO-B1.0 survey (Monet et al. 2003): the star 1351–0294859 is at $18^{\rm h}16^{\rm m}35\overset{\rm s}{.}93$, $+45^\circ10'34\overset{''}{.}2$. This is $0\overset{''}{.}4$ from the radio position, reasonably consistent with typical astrometric accuracy from the USNO catalog. However, the mean epoch of those data is 1974, so a small proper motion could also account for some of the difference. The photometry for this source is presented in Table 1, where we have assumed uncertainties of 0.2 mag for the Digitized Sky Survey (DSS) photometry.

The same source is identified in the Catalina Surveys Data Release 1 (CSDR1; Drake et al. 2009) Catalina Real-Time Transient Survey (CRTS). The automated software actually identified *two* sources that make up the counterpart: CSS J181635.9+451033 and CSS J181635.9+451036. These sources are quite close ($<2\overset{''}{.}5$ apart, which is comparable to the plate scale of the instrument) and they both have the same average magnitude of $V_{\rm CSS} \approx 18.4$ mag, measured with an unfiltered detector. There were no images where both sources were seen at the same time, and comparing the positions of individual detections (rather than the average positions in the catalog), it seems they are the same source that was split by the photometric pipeline into two. The photometry of the combined source (106 measurements over 6.5 yr, from 2005 May to 2011 November) is largely consistent with being constant, except for eight points. Three of those are clearly when the software misidentified a slightly brighter ($V_{\rm CSS} \approx 16.5$ mag) star about $10''$ to the southeast (visible in Figure 2) as being part of this object. The others are not as easy to reject, but since they also have $V_{\rm CSS} \approx 16.5$ mag, we think it likely that it was another misidentification or a photometric artifact; without the images we cannot be certain. Excluding those eight points we have data consistent with a constant $V_{\rm CSS} = 18.47$ mag with root-mean-square variations of 0.18 mag. The χ^2 relative to a constant model is slightly high (156.1 for 97 degrees of freedom), but is similar to that for a star of similar brightness $30''$ away. There is no evidence for any secular trends in the photometry. The uncertainty on the mean magnitude is about 2 mmag, but for absolute photometry we transform from the unfiltered instrumental magnitude to Cousins V by $V = V_{\rm CSS} + 0.31(B-V)^2 + 0.04$ with a scatter of 0.06 mag.[15] Since this object has very nearly $B - V \approx 0$ (this assumes that the colors are constant over time and orbital phase), we find

[15] See http://nesssi.cacr.caltech.edu/DataRelease/FAQ.html.

Table 1
Photometry of the Optical Counterpart to PSR J1816+4510

Band	FUV	NUV	*u*	*B*	*V*	*R*	*R*	*I*
Magnitude	19.86 ± 0.18	19.11 ± 0.09	18.52 ± 0.04	18.3 ± 0.2	18.51 ± 0.06	18.4 ± 0.2	18.27 ± 0.04	18.4 ± 0.2
Wavelength (nm)	152	230	345	438	545	641	641	798
Source	*GALEX*	*GALEX*	*Swift*	DSS	CSDR1	DSS	WIYN	DSS
System	AB	AB	AB	Vega	Vega[a]	Vega	Vega	Vega

Notes. For each measurement, we give the measured magnitude with uncertainties (assumed to be 0.2 mag for the DSS), the approximate central wavelength, the origin (telescope/survey), and whether the magnitude is on the AB or Vega system.
[a] This was transformed from the unfiltered detector system assuming $B - V = 0$.

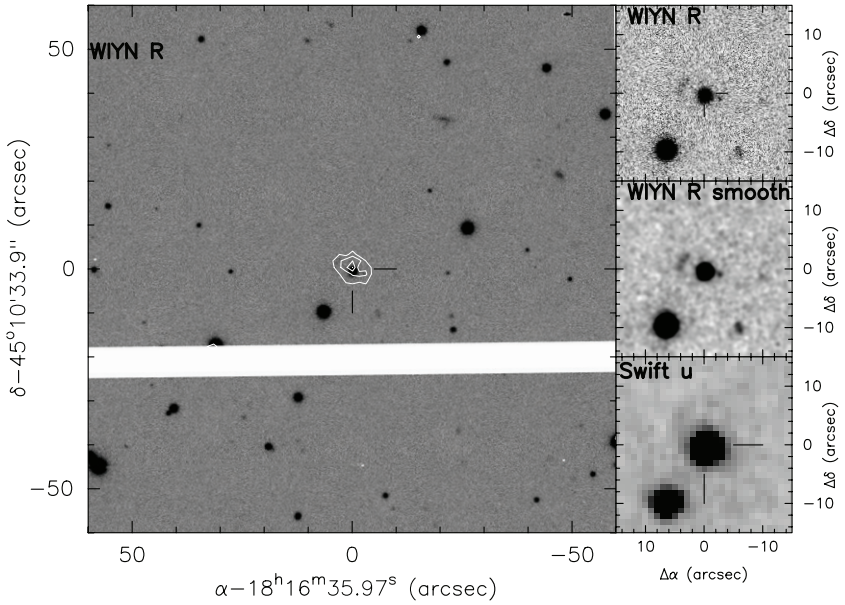

Figure 2. Optical images of the PSR J1816+4510 field. The radio position is indicated with the tick marks, and the uncertainties are dominated by uncertainties in the absolute astrometry of the optical data. The large image is the WIYN MiniMo *R*-band data, showing a $2' \times 2'$ portion. The white band is the gap between the MiniMo CCDs. The contours are from the *GALEX* near-UV image, and the source GALEX J181635.9+451034 is consistent with a point source. The insets on the right are (top to bottom): the WIYN MiniMo *R*-band data zoomed to show a $30'' \times 30''$ portion and with a gray scale adjusted to show the faint structure; the WIYN MiniMo *R*-band data smoothed with a Gaussian kernel with $\sigma = 2$ pixels ($0\farcs28$); and the *Swift* UVOT *u*-band image.

$V = 18.51 \pm 0.06$, although this uncertainty may be somewhat underestimated.

We then identified the same source in the *Galaxy Evolution Explorer* (*GALEX*) All-sky Imaging Survey (AIS; Morrissey et al. 2007) database. Here, the source is GALEX J181635.9+451034 and its position is offset by $0\farcs4$ relative to the radio position, which is consistent with the median offset of $1''$ found for *GALEX*.[16] Again, photometry is presented in Table 1.

In the USNO source catalog, the average density of sources brighter than $R = 18.4$ mag is 6.1×10^{-4} arcsec^{-2}, so the false association rate given the measured source offset is 3×10^{-4}, making it very likely that we have the correct counterpart. Moreover, the presence of a *GALEX* source at the same position with a significant far-UV (FUV; 152 nm) detection makes it essentially certain: there are only four FUV detections with magnitudes brighter than 19.9 mag within a $10'$ radius, so the false association rate is 2×10^{-6}. As we will see below, this source is so bright and blue that it is rather unusual, making the chance of finding one within $0\farcs5$ of the radio position by chance extremely low.

We then identified an observation with the *Swift* satellite (Observation ID 00041440003). We see a bright source at the radio position in the data from the Ultraviolet and Optical Telescope (UVOT; Roming et al. 2005). The observation was on 2010 August 4, and consisted of eight separate integrations in the *u* filter (central wavelength of 3450 Å) spread over 11 hr with a total integration of 3173 s and 2×2 pixel binning. We determined both time-resolved and summed photometry from these data using *Swift* data-reduction tools. First, we ran the task `uvotsource` on each separate observation (along with respective exposure maps) to measure how bright the object was in each individual integration (with the 2011 October 31 calibration database). We then summed the integrations using `uvotimsum` and measured the summed magnitude using `uvotsource`, where in both cases the source region was a circle with $5''$ radius centered on the radio position and the background region is $25''$ in radius centered near the pulsar but not including any visible sources. The best-fit position of the source is $18^{\rm h}16'35\farcs93$, $+45^\circ10'34\farcs0$, or $0\farcs12$ away from the radio position. This is without any additional boresight correction beyond that applied by the *Swift* processing. The final detection significance in the summed image was 72.8σ, but our photometry includes the suggested systematic uncertainty of 0.02 mag in addition to the statistical uncertainty.

[16] See http://galexgi.gsfc.nasa.gov/docs/galex/Documents/ERO_data_description_2.htm.

In Figure 1, we show the measured *Swift* and CRTS photometry as a function of orbital phase, where the *Swift* observation times have been corrected to the solar system barycenter using the `barycorr` task, and the CRTS observation times have been corrected to the heliocenter using the `rvcorr` task in `IRAF` (for an 8 hr orbit, the differences between helio- and bary-center are negligible). The *Swift* data are consistent with no variations, with $\chi^2 = 5.4$ for 7 degrees of freedom. Each individual measurement can largely be considered instantaneous, as the exposure times are at most 800 s compared to an observation duration of 11 h and an orbital period of 8.7 h. The rms scatter of the data about the mean is 0.05 mag. The CRTS data have been binned, with between 2 and 16 individual observations averaged into each point. There may be a trend with orbital phase, such that the data are slightly (15%) fainter near phases[17] of 0.75, but while formally significant ($\chi^2 = 29.2$ for 14 degrees of freedom), we do not know the level of systematic uncertainties due to artifacts and misidentifications. There were no measurements in the bin just before the apparent flux minimum, but without the raw data we cannot say whether there were no observations or just no detections. The rms scatter of the data about the mean is 0.08 mag. The possible trend in the CRTS data is not necessarily seen in the *Swift* data, although it is difficult to be certain.

2.2. New Optical Data

We observed PSR J1816+4510 using the Mini-Mosaic Imager (MiniMo) on the 3.5 m Wisconsin Indiana Yale NOAO (WIYN) telescope (Saha et al. 2000). The data were a 300 s exposure in the Harris-*R* filter on 2011 March 24 taken shortly before sunrise. Seeing was 0.″7, with a plate scale of 0.″14 pixel^{-1}. The data were corrected for bias level and flatfielded using standard procedures in `MIDAS`. The image was registered to the International Coordinate Reference Frame (ICRF) using 130 Two Micron All Sky Survey (2MASS; Skrutskie et al. 2006) stars, giving fits with rms residuals of 0.″2 in each coordinate. We did photometric calibration using an observation of the Landolt 98 field (Stetson 2000) earlier in the night, determining a zero point using 22 stars; we estimate a zero-point uncertainty of 0.03 mag. As in the other data, there was a bright source at the position of the pulsar, but here the position offset was only 0.″02. We measured the object using `sextractor` (Bertin & Arnouts 1996), with the same settings that we used for the standard stars. In addition to the potential counterpart, we see some faint structure to the northeast and southwest, at distances of 2″–4″. This may just be some faint stars near the detection limit of the image, but they are also somewhat suggestive of an Hα bow shock nebula such as that seen around the black-widow system PSR B1957+20 (Kulkarni & Hester 1988) or around the non-interacting pulsar/white dwarf binary PSR J0437−4715 (Bell et al. 1995). Images of both the WIYN and *Swift* data are shown in Figure 2.

2.3. Optical/Ultraviolet Spectral Energy Distribution

The potential counterpart of PSR J1816+4510 is very blue compared to nearby sources. In Figure 3, we show a color–magnitude diagram using the *R*-band and *u*-band data, where the counterpart is roughly 1 mag bluer than the field sources. Just the *u* and *R* data indicate a rather hot blackbody, although since the reddening vector is roughly parallel to the track of a blackbody, the temperature and reddening are degenerate. However, some temperature above 10,000 K is required.

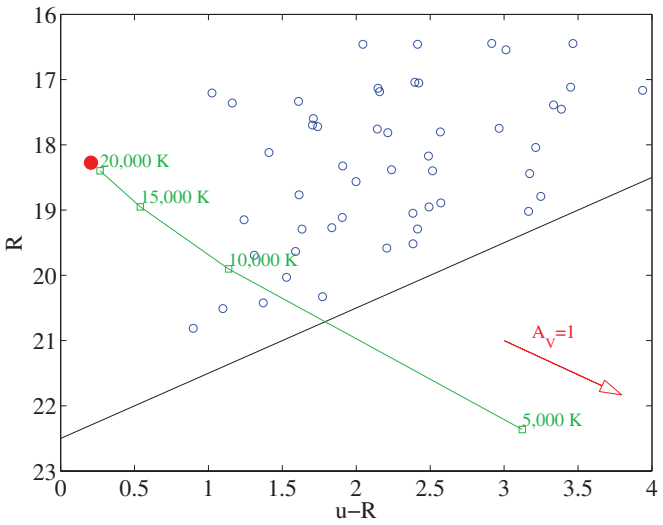

Figure 3. Color–magnitude diagram for the sources in the WIYN *R*-band and *Swift* *u*-band images. The source at the position of the pulsar is the filled circle. The black line is the approximate $u = 22.5$ detection limit of the UVOT image. We show the results of a reddened ($A_V = 1$ mag) blackbody model for the temperatures shown, with a size of 0.005 $R_\odot/100$ pc. A reddening vector showing 1 mag of extinction is also shown.

(A color version of this figure is available in the online journal.)

We fit all of the optical/UV photometry to determine the SED of this source. For the data in the Vega system, we used zero-point fluxes from Bessell et al. (1998). We then convolved various model SEDs with filter transmission curves and compared the resulting fluxes with those derived from the data. For the DSS and CSS data, we assumed standard Johnson *BRI* filters, and this is clearly a simplification, but the large uncertainties for DSS mean that those data have modest weight. For the WIYN data, we used a filter curve from Kotulla et al. (2009); for the *Swift* data, we used a response file from the *Swift* Web site[18]; the *GALEX* filters were from the COSMOS Web site.[19] We used a nominal extinction curve from Cardelli et al. (1989) and O'Donnell (1994), with a reddening ratio $R_V = 3.1$.

Our first model was a reddened blackbody. We got a good fit, with $\chi^2 = 6.4$ for 5 degrees of freedom (and this includes the poorly calibrated DSS data). The best-fit model had $T_{\rm eff} = 18{,}000$ K, $A_V = 0.77$ mag, and size $R = 0.1\ R_\odot$ at a nominal distance of 2 kpc, but a wide range of solutions had similarly good fits (Figure 4), with larger temperature requiring larger extinctions and smaller radii; as in Figure 3, this is largely the result of the blackbody model between the *u* and *R* data being parallel to the reddening vector. The size is largely determined from the WIYN observation, with

$$\log_{10}\left[\left(\frac{R}{R_\odot}\right)\left(\frac{2\,\mathrm{kpc}}{d}\right)\right] \approx -0.54 - 0.35\log_{10}\left(\frac{T_{\rm eff}}{10^3\,\mathrm{K}}\right)$$

$$A_V \approx -3.09\log_{10}\left(\frac{T_{\rm eff}}{10^3\,\mathrm{K}}\right)^2 + 10.65\log_{10}\left(\frac{T_{\rm eff}}{10^3\,\mathrm{K}}\right) - 7.72$$

along the best-fit locus.

[17] Note that for pulsars' ephemerides, conjunctions occur at phases of 0.25 and 0.75 with 0.75 having the pulsar between the companion and the observer.

[18] http://heasarc.nasa.gov/docs/swift/proposals/swift_responses.html.

[19] http://www.astro.caltech.edu/~capak/cosmos/filters/.

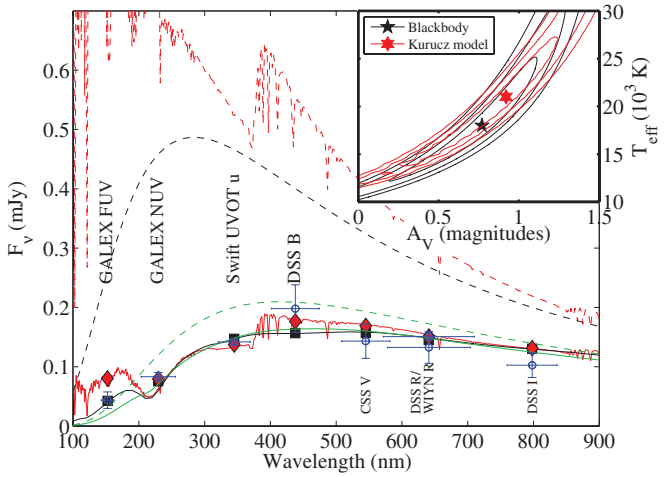

Figure 4. Results of fitting to the broadband photometry from Table 1. We plot the best-fit SEDs, with the blackbody model (black) and model atmosphere (red). The solid curves have had extinction applied, while the dashed curves are without extinction. The black squares and red diamonds are the respective model SEDs convolved with the filter passbands, while the circles are the data. The inset shows contours of χ^2 vs. extinction A_V and effective temperature $T_{\rm eff}$ for the blackbody models (black) and model atmospheres (red). Contours are at 1σ, 2σ, and 3σ confidence on the joint fit. The stars represent the best-fit parameters for each model. For comparison, we also plot the best-fit blackbody with $A_V = 0.2$ mag (green).

(A color version of this figure is available in the online journal.)

We then fit model stellar atmospheres from Kurucz (1993). We used models with gravity $10^4\,{\rm cm\,s^{-2}}$, although the results were not sensitive to this. The best-fit model was slightly hotter than the best-fit blackbody (21,000 K, with $A_V = 0.92$ mag and $R = 0.12\,R_\odot$ at a distance of 2 kpc), and had a slightly worse χ^2 (11.5), but uncertainties in the extinction law below 250 nm (Cardelli et al. 1989) could change the result; the most discrepant point was the *GALEX* FUV observation. The best-fit region in the $(A_V, T_{\rm eff})$ plane is very similar to that of the blackbody (Figure 4). We also tried a 15,000 K white dwarf atmosphere model (a DA white dwarf with hydrogen on the surface, which is expected for such a hot star; Hansen & Liebert 2003), kindly supplied by D. Koester. The fit was similar to that of a 15,000 K main-sequence star since the main differences (the stronger Balmer absorption sequence in the white dwarf) are not easily distinguished with the available DSS *U*-band photometry; the white dwarf model also had trouble fitting the *GALEX* FUV point.

An absorbed power-law spectrum such as that of an active galactic nucleus does not fit ($\chi^2 = 34.7$ for 5 degrees of freedom). While the spin-down and radio emission of PSR J1816+4510 indicate that no accretion disk is likely present (cf. Archibald et al. 2009), given the unusual nature of the optical/UV emission it may be worth considering whether the high temperature that we measure is from an accretion disk around the pulsar, where ultraviolet emission is common (although this would tend to also have bright X-ray emission which we do not see, the X-rays could be variable). The SED that we measure is consistent with a single-temperature blackbody, not a multi-temperature model as is usually used to model accretion disks (Shakura & Sunyaev 1973; Vrtilek et al. 1990). Therefore, while we cannot rule out such a model using photometry alone, we consider it unlikely. Spectroscopy should be definitive.

We note that the faint, diffuse emission seen in the *R*-band image could have contaminated some of the lower-resolution data (in particular *Swift* and *GALEX*). However, at least at the *R* band, the brighter spot (to the southwest) is about 100 times fainter than the star, so assuming a similar spectrum (which is conservative for the bluer bands, as the emission is probably either Balmer dominated or stellar) it is unlikely to be important at the >1% level. We tried subtracting the stellar point-spread function (PSF) at the position of the counterpart, but do not see any significant residual emission beyond that visible in Figure 2.

3. X-RAY AND γ-RAY DATA AND ANALYSIS

3.1. Swift X-ray Data

In the 2.8 ks photon-counting observation with X-ray Telescope (XRT; Burrows et al. 2005), zero counts were detected in a circle with a radius of 20″ around the radio position. Millisecond pulsars typically have a combination of X-rays from thermal (from hot polar caps) and non-thermal (either magnetospheric, or from a shocked pulsar wind) spectra (e.g., Zavlin 2007). The thermal components have blackbody temperatures with $kT \approx 0.1$–0.2 keV and luminosities of $\sim 10^{-3}\dot{E}$ (Zavlin 2007; Possenti et al. 2002). For more energetic pulsars, the non-thermal components dominate, and these are typically fit as power laws with photon indices $\Gamma \approx 1.5$ and again luminosities of $\sim 10^{-3}\dot{E}$. Based on a power law with a photon index of 1.5, we set a 2σ limit of $\lesssim 3\times10^{-15}\,{\rm erg\,s^{-1}\,cm^{-2}}$ for the unabsorbed 0.5–10 keV flux from PSR J1816+4510 for absorption column densities $N_{\rm H}$ in the range of $10^{20}\,{\rm cm^{-2}}$–$10^{21}\,{\rm cm^{-2}}$ (corresponding to $A_V = 0.06-0.6$ mag, based on Predehl & Schmitt 1995). For a measured spin-down luminosity of $\dot{E} = 5\times10^{34}\,{\rm erg\,s^{-1}}$ (although see below for possible corrections to this), our limit then corresponds to $L_{\rm X,non-th} \lesssim 3\times10^{-4} d_2^{-2}\dot{E}$. We can do the same computation for a thermal spectrum, with unabsorbed flux limits of $(9$–$17)\times10^{-15}\,{\rm erg\,s^{-1}\,cm^{-2}}$ (0.5–2 keV) for a blackbody with $kT = 0.15$ keV and $N_{\rm H} = (1$–$10)\times10^{20}\,{\rm cm^{-2}}$. This then gives a similar limit of $L_{\rm X,thermal} \lesssim 2\times10^{-4} d_2^{-2}\dot{E}$. Both of these efficiencies are low but not outside the observed range (Zavlin 2007; Ransom et al. 2011), and suggest that the X-ray flux may only be slightly below the *Swift* limit.

3.2. Fermi Data

The radio position of PSR J1816+4510 matches almost exactly with a source from the *Fermi* Large Area Telescope Second Source Catalog (2FGL; The Fermi-LAT Collaboration 2011). The source 2FGL J1816.5+4511 (1FGL J1816.7+4509 from the first-year catalog) is 1.4′ away from PSR J1816+4510, with a position uncertainty of ≈5′ in radius. It is listed as having a power-law spectrum with a photon index of $\Gamma = 2.11 \pm 0.08$ ($N_E \propto E^{-\Gamma}$), and 0.1–100 GeV flux of $(15.3 \pm 1.8)\times10^{-12}\,{\rm erg\,s^{-1}\,cm^{-2}}$.

However, there is another year of data available in the *Fermi* archive, and we wished to do further spectral analysis and look for pulsations. Therefore, we analyzed data from the *Fermi* Large Area Telescope (LAT; Atwood et al. 2009), including events from 2008 August 5 to 2012 January 19. We followed standard procedures[20] in filtering events, selecting those with event class 2 within a 10° radius around PSR J1816+4510, with energies between 0.2 and 10 GeV (to avoid the poor PSF at the lowest energies; the pulsar did not appear to be detected there anyway) and zenith angles <105°. We computed the spectrum using an unbinned likelihood analysis,[21] including the

[20] See http://fermi.gsfc.nasa.gov/ssc/data/analysis/scitools/data_preparation.html.
[21] See http://fermi.gsfc.nasa.gov/ssc/data/analysis/scitools/likelihood_tutorial.html.

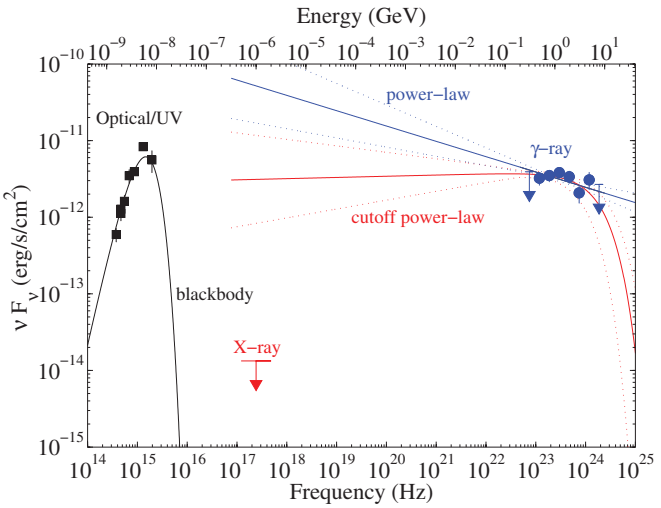

Figure 5. SED of PSR J1816+4510 and its presumed companion, from the optical to γ-rays. We show the optical/UV photometry along with the best-fit blackbody model, both corrected for reddening with $A_V = 0.2$ mag. The X-ray upper limit is based on the *Swift* XRT non-detection. The γ-ray points were derived from fitting a power-law model to each individual energy bin, and we show the best-fit single power-law and cutoff power-law models along with $\pm 1\sigma$ uncertainties.

(A color version of this figure is available in the online journal.)

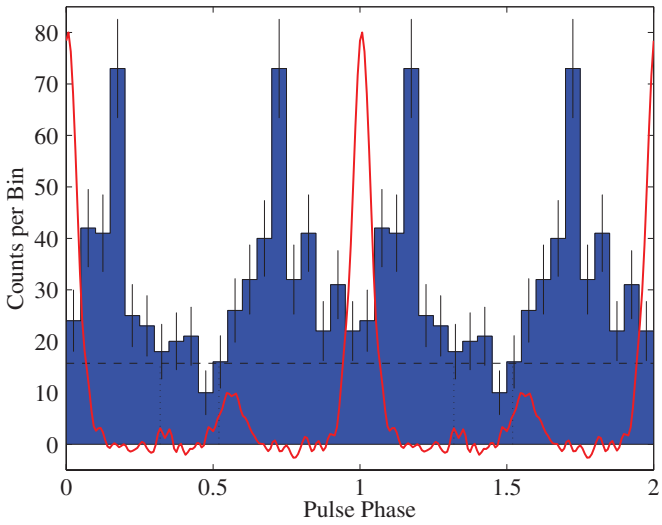

Figure 6. Pulsed γ-ray light curve of 2FGL J1816.5+4511, determined from all LAT data in the 0.3–10 GeV range up to 2012 January and repeated twice for clarity. We used the radio ephemeris to initially identify the pulsar, but then refined the ephemeris using the *Fermi* data since they have a longer time span. The dashed horizontal line is the approximate background level based on the phases indicated by the vertical dotted lines. The red trace is the radio pulse profile, based on 820 MHz data from the Green Bank Telescope (K. Stovall et al. 2012, in preparation), arbitrarily scaled.

(A color version of this figure is available in the online journal.)

contributions of sources out to a radius of 17° from the 2FGL catalog as well as isotropic and Galactic background models appropriate for pass 7 data (models `iso_p7v6source.txt` and `gal_2yearp7v6_v0.fits`) with the `P7SOURCE_V6` instrument response, although we held most of the source parameters fixed at their catalog values with the exceptions of those sources within 8° of PSR J1816+4510 and the diffuse background normalizations. Photons are significantly detected between 0.5 GeV and 5 GeV. For 2FGL J1816.5+4511, we find a good fit with a power-law model with a photon index of $\Gamma = 2.20 \pm 0.07$ and a normalization of $(1.5 \pm 0.1) \times 10^{-12}$ cm^{-2} s^{-1} MeV^{-1} at 1.15 GeV giving an integrated 0.1–100 GeV flux of $(19.6 \pm 1.5) \times 10^{-12}$ erg s^{-1} cm^{-2}, with a Test Statistic of 404 (i.e., roughly a 20σ detection); this is similar to the result from the 2FGL catalog. We do not incorporate any systematic uncertainties related to calibration errors.

We repeated the spectral fit with a power law modified by an exponential cutoff, $N_E \propto E^{-\Gamma} e^{-E/E_c}$. The meager energy range with significant detections meant that the cutoff could not be strongly constrained, but we find $\Gamma = 2.0 \pm 0.1$, normalization $(7.9 \pm 0.8) \times 10^{-12}$ cm^{-2} s^{-1} MeV^{-1} at 0.55 GeV, and a cutoff energy of $E_c = 7.5 \pm 4.0$ GeV; the integrated flux was $(15 \pm 3) \times 10^{-12}$ erg s^{-1} cm^{-2}. Formally, this fit was statistically equivalent to the pure power-law fit, and other local minima were also possible depending on where the fit was started. We note that the parameters we find are outside the range of most millisecond pulsars, with Γ and E_c both higher than are typical. Much of this comes from the highest energies we included in our fit (4–6 GeV; Figure 5). Without this bin, a fit with more typical values ($\Gamma \approx 1.5$, $E_c \approx 3$ GeV) is acceptable. We show the fits in Figure 5, where γ-ray fluxes were determined from modeling the flux in each energy bin as a single power law[22] using the contributed task `likeSED`. We therefore urge caution in interpreting the γ-ray spectrum.

For the pulsation search, after the initial event filtering, we assigned phases to all of the events using the best-fit radio ephemeris using the *Fermi* plugin for `tempo2`[23] (Hobbs et al. 2006). We detected pulsations using the initial radio ephemeris, but given the longer time span of the *Fermi* data compared to the radio data (1262 days versus 320 days), we were able to refine the radio ephemeris (in particular the spin-down), as discussed in Stovall et al. We then used the refined ephemeris to update the event phases. Selecting the 632 events $\leqslant 0.^{\circ}65$ from the radio position and with energies between 0.3 GeV and 10 GeV (optimizing those parameters for the pulse amplitude, as in Ransom et al. 2011), we see very significant pulsations, with an H-test statistic (de Jager et al. 1989) of 64.4 for 11 harmonics (false alarm probability of 4×10^{-23}). With this solution, we see clear pulsations in the binned light curve with $\chi^2 = 157$ for 19 degrees of freedom. The pulsations have two sharp peaks separated by slightly less than one half of a cycle (Figure 6) similar to the radio pulse. Selecting events from phases 0.32–0.52 (where the pulse is at a minimum), we see a radial profile that is consistent with being flat in terms of counts per unit area out to 2°, with an implied background rate over all phases of 237 ± 38 deg^{-2} (the horizontal line in Figure 6). This would mean that our light curve is consistent with being 100% pulsed. Averaging over pulse phase, the count rate was roughly constant as a function of orbital phase (Figure 1), with $\chi^2 = 20.9$ for 15 degrees of freedom. Over the two years of the 2FGL catalog, the light curve was likewise consistent with being constant on month timescales ($\chi^2 = 22.1$ for 23 degrees of freedom, based on the 2FGL variability index).

4. DISCUSSION

Based on the *Fermi* flux of 20×10^{-12} erg cm^{-2} s^{-1} (0.1–100 GeV), we find a γ-ray luminosity of $1 \times 10^{34} d_2^2$ erg s^{-1}.

[22] See http://fermi.gsfc.nasa.gov/ssc/data/analysis/scitools/python_tutorial.html.

[23] See http://fermi.gsfc.nasa.gov/ssc/data/analysis/scitools/pulsar_analysis_appendix_C.html.

We determine the γ-ray efficiency by comparing this with $\dot{E}$ and find $\eta_\gamma \equiv L_\gamma/\dot{E} = 0.19 d_2^2$ assuming no geometric beaming correction; this is comparable with that found for purely magnetospheric emission from millisecond pulsars with *Fermi* (Abdo et al. 2009; Ransom et al. 2011). We can set a weak upper limit to the distance by requiring $L_\gamma \leqslant \dot{E}$, which gives $d_2 \lesssim 2.3$ ($d \lesssim 4.6$ kpc). Given the highly pulsed γ-ray light curve, it is possible that all of the emission could be magnetospheric in origin like for most millisecond pulsars, but some might still be related to intra-binary shocks such as in the PSR B1259−63 system (Abdo et al. 2011, which is not a millisecond pulsar but has a hot companion like that seen here), especially if there are contributions from inverse Compton scattering off the UV photons present in both cases.

In Figure 5, we plot the SED from optical to γ-rays. Energetically, the optical/UV are almost as important as the γ-rays, which would make it difficult for them to both ultimately come from $\dot{E}$ (as the γ-rays already require a substantial fraction of $\dot{E}$), supporting a hot companion which radiates on its own. Changing the extinction to a lower value such as $A_V = 0.2$ mag (see below) reduces the total optical luminosity somewhat, but it is still substantial. The simple power-law fit to the γ-rays exceeds the X-ray upper limit (much as in Durant et al. 2011), but the cutoff power law does as well, so with either model we might need a spectral break between 1 keV and 100 MeV. However, our spectral fitting only had a limited number of counts, and we did not include systematic uncertainties related to instrumental calibration. The apparent discrepancy between the γ-ray emission and the X-ray upper limit may only be a consequence of the spectral fit; the ratio of $\sim 10^3$ between the γ-ray and X-ray luminosities is reasonable for other millisecond pulsars (Ransom et al. 2011; Takata et al. 2012).

In what follows, we primarily assume that the optical/UV emission come from a single photosphere that is the companion of the pulsar in a binary system. However, without a spectrum, we cannot exclude contributions from shocked plasma—this might help explain some of the slightly discrepant UV data points or the somewhat high extinction (see below).

Given our extremely likely detection of the optical/UV companion of PSR J1816+4510 and the identification of the pulsar at γ-ray energies, we consider how this system fits among the known recycled pulsars with low-mass companions. Some of the implications of this system are common to a wide range of similar systems, but the uniquely hot temperature may point to either a fortuitous detection of a short-lived evolutionary state or a different evolutionary path.

At the nominal distance, our optical photometry implies $R = 0.1 d_2\, R_\odot$ ($L_{\rm optical/UV} \approx L_\odot$). If the optical companion filled its Roche lobe, then it would be at a distance of 10 kpc, which is not impossible given the radio and γ-ray properties but is unlikely (it would require $L_\gamma \approx 4\dot{E}$, but this constraint is based on isotropic emission). If the optical source is an unrelated object, then it would either be a nearby white dwarf at $\lesssim$300 pc (Fontaine et al. 2001[24]; we take it as a 0.6 $M_\odot$ carbon/oxygen white dwarf) or a main-sequence star (B3–5) at a distance of 70–100 kpc (Cox 2000); while the former is possible, main-sequence stars with $M \gtrsim 3\, M_\odot$ would not be expected at such distances.

Our best-fit value for the extinction A_V is 0.5–1.0 mag. This is larger than the largest value in this direction (≈0.2 mag) determined by Drimmel et al. (2003), and Schlegel et al. (1998) give a similar result. Given the limitations of our fit, values of $\lesssim$0.2 mag are not excluded but would imply effective temperatures of ≈12,000 K ($A_V = 0.2$ mag increases χ^2 by 2.2 over the best-fit value for the blackbody fit), and we plot the best-fit $A_V = 0.2$ mag blackbody for comparison in Figure 4. To evaluate the likely extinction, we determined our own run of extinction with distance by examining all of the 2MASS stars within 1° and finding the red clump (Drimmel et al. 2003; Durant & van Kerkwijk 2006). While we cannot determine the extinction as close as 2 kpc (there are not enough stars), we measure extinctions of ≈0.6 mag for distances $\geqslant$5 kpc, which is reasonably consistent with our SED fitting. At this Galactic latitude ($b = +24.^\circ 7$), much of the extinction will be close to the Sun, so the value measured at 5 kpc should be applicable to closer objects. We note that our value of $A_V \gtrsim 0.5$ mag is actually consistent with the measured DM, assuming an ionized fraction of 10% and the usual (Predehl & Schmitt 1995) conversion between extinction and hydrogen column density, but the hydrogen column density interpolated from H I maps[25] is lower, 4×10^{20} cm^{-2}. Optical and X-ray spectroscopy can hopefully narrow down the possible range of the extinction.

With a minimum eclipse duration of 7% of the orbit at 820 MHz (K. Stovall et al. 2012, in preparation), the eclipsing radius is ≈0.5 $R_\odot$. This is similar to the Roche lobe radius, suggesting that some of the eclipsing material may be gravitationally bound to the companion star, although the tail of delayed times of arrival (TOAs) extends to larger radii. The maximum delay observed at 820 MHz (about 400 μs) implies an excess dispersion measure of 0.06 pc cm^{-3}, or an electron column density of $N_e \approx 2 \times 10^{17}$ cm^{-2}. If this material is distributed over 0.5 $R_\odot$, then we would have an electron density $n_e \approx 6 \times 10^6$ cm^{-3}. Assuming that the material is moving at the escape velocity, we estimate a mass-loss rate of $\dot{M} \sim 10^{-13}\, M_\odot$ yr^{-1}, so the companion would not be substantially diminished over a Hubble time (similar to Stappers et al. 1996). Such a mass-loss rate is actually comparable with expectations for radiative winds from more massive sdB stars with (presumably) similar surface gravities[26] (Vink & Cassisi 2002; Unglaub 2008). If this and not ablation (which would only require 0.1% of $\dot{E}$) is the origin of the mass loss, then the low gravity and high temperature of the companion seem to be necessary components for the ionized gas eclipses as winds cease for gravities $>10^6$ cm s^{-2} and temperatures <20,000 K (Unglaub 2008). While minor in terms of mass loss, the winds might be nonetheless important evolutionarily in altering the diffusive equilibrium (Unglaub & Bues 1998), and hence the atmospheric appearance and onset of shell burning.

The measured effective temperature of $\gtrsim$15,000 K is far hotter than the companion to any known black-widow or redback system (typically $\lesssim$6000 K; van Kerkwijk et al. 2005; Pallanca et al. 2010; R. P. Breton et al. 2012, in preparation; C. Bassa 2011, private communication) by a factor of almost three. Pulsars with hot white-dwarf companions are known (e.g., 8,550 K for PSR J1012+5307, 10,090 K for PSR J1911−5958A, and 15,000 K for PSR B0820+02; van Kerkwijk et al. 2005 and references therein), but they do not have broad eclipses like those we see here. We can then address the peculiarity of this system in two ways: (1) if this is an interacting binary system, then what would be the consequences of it being so hot, and (2) why is it so hot?

[24] Also see http://www.astro.umontreal.ca/~bergeron/CoolingModels/.

[25] Using http://asc.harvard.edu/toolkit/colden.jsp.

[26] Although we are outside their nominal luminosity range and near the low end of the temperature range usually considered, the surface gravities are similar so the winds are likely to be similar.

For the first question, if we treat PSR J1816+4510 as an interacting binary regardless of origin, it is not surprising that we do not see any modulation of the *u*-band light curve: the additional energy deposited by the pulsar has an equilibrium temperature of $\lesssim(\dot{E}/4\pi a^2\sigma)^{1/4} \approx 7000$ K (for an efficiency of 100%, while typical efficiencies are closer to 15%; R. P. Breton et al. 2012, in preparation). Note that this ascribes all of the observed spin-down $\dot{P} = 4.1 \times 10^{-20}\,\mathrm{s\,s^{-1}}$ to magnetic dipole radiation and not to secular (i.e., Shklovskii 1970) acceleration; with a typical millisecond pulsar velocity of $v = 100 v_{100}\,\mathrm{km\,s^{-1}}$, the secular $\dot{P}$ would be $1.7\times10^{-21} v_{100}^2 d_2^{-1}\,\mathrm{s\,s^{-1}}$ or 4% of the measured value, so it is likely that the $\dot{E}$ value we use above is close to correct (corrections due to differential Galactic acceleration are even smaller; Nice & Taylor 1995). Since the implied temperature is so low compared to the observed temperature, we would expect the illuminated side to be $\lesssim$5% brighter than the dark side (for an effective temperature of 15,000 K), which is the level of the observed scatter in the *Swift* photometry; if the orbital modulation of the CRTS data is real, then it is difficult to understand its amplitude. We note that our SED fitting assumes that the data are constant with time and are defined by only a single model, and these are not necessarily valid assumptions. Even aside from the lack of strong orbital modulation, there could also be secular/state changes such as those seen in PSR J1023+0038 (Archibald et al. 2009). However, the limit on secular evolution from the CSDR1 data (which span the times of the *GALEX*, *Swift*, and WIYN photometry) suggests that most of the data are consistent with a single model. In the future, single-epoch photometry should be able to resolve this question. The nominal radius of the companion is well within the typical range for black-widow/redback companions in the field (sources in globular clusters often are considerably $> R_\odot$; Ferraro et al. 2001; Cocozza et al. 2008; Pallanca et al. 2010), which may be some clue to the formation mechanism. However, unlike some of those systems, it is likely a factor of several smaller than the Roche lobe, so the companion may not be significantly distorted.

It may be that the $0.5\,R_\odot$ eclipse duration is set not by the Roche lobe radius but by the intrabinary shock radius between the $\dot{E}$-driven wind and the companion (Arons & Tavani 1993), where the shock represents the equilibrium between the relativistic wind of the pulsar and the presumed radiation-driven wind from the companion. Assuming an electron density of $\sim10^7\,\mathrm{cm^{-3}}$ and pure hydrogen composition at a radius of $R_{\rm shock} \approx 0.5\,R_\odot$, the ram pressure $\rho v^2/2$ is 0.03 dyne cm^{-2} for a wind at the escape velocity, which is a factor of $\sim$200 less than $\dot{E}/(4\pi c(a - R_{\rm shock})^2)$; if this model is valid, then we must consider that the wind might be moving faster than the escape speed (Phinney et al. 1988; Unglaub 2008), our density might be too low (in particular the material might be clumpy), or possibly only a fraction of $\dot{E}$ participates in the shock (Stappers et al. 2003).

For the second question, we can ask why the companion would be so hot. First, it is possible that PSR J1816+4510 has a normal cool companion, but that the optical/UV flux comes from another source. This could be a star, either as part of a triple system or an unrelated object. Having an unrelated object seems highly unlikely given the positional coincidence, and an association between the radio, γ-ray, and optical sources is the most likely explanation, but without optical modulation to confirm we cannot be certain. A triple system can largely be ruled out by the 3 yr span of the *Fermi* timing, as those data are consistent with only the 8 hr binary. As mentioned before, emission from shocked plasma is also possible.

Without knowing the surface gravity (and hence having some idea of how degenerate the companion is), any inferences about why the companion is so hot are difficult. For helium-core white dwarfs in the mass range considered here ($\lesssim0.2\,M_\odot$), burning of a thick shell of hydrogen (Webbink 1975) can keep the sources hotter for considerably longer (Gyr; Sarna et al. 2000; Panei et al. 2007; Steinfadt et al. 2010) than standard cooling would allow (cf. Lorimer et al. 1995), but the temperatures tend to be $\lesssim$10,000 K; more massive white dwarfs can stay at $>10^4$ K for longer, and unstable hydrogen flashes can also push the temperature above 10^4 K for more massive white dwarfs temporarily. We note, though, that the recently discovered binary SDSS J065133.33+284423.3 (Brown et al. 2011) has a helium-core white dwarf at a similar temperature to what we find, and this source is somewhat more massive ($0.25\,M_\odot$) than the expected burning limit, although the limit is metallicity-dependent and the contribution of tidal heating in this system is unknown. If the companion of PSR J1816+4510 were a normal white dwarf, then we would expect PSR J1816+4510 to be on the low side of the possible distances (radii of $\lesssim0.05\,R_\odot$ are typical at these masses; Panei et al. 2007) with an age of $\lesssim$0.5 Gyr. In this scenario, PSR J1816+4510 would be the first pulsar/white dwarf system with ionized-gas eclipses. However, it could also be that the companion is still hotter and younger still if it has not yet equilibrated from a common-envelope evolutionary phase (Paczynski 1976) or Roche lobe overflow that stripped away the outer layers of the companion, leaving it hot, large, and in a circular orbit (e.g., Driebe et al. 1998). For low-mass ($<0.2\,M_\odot$) white dwarfs, the residual hydrogen burning typically results in luminosities of $<0.1\,L_\odot$ (Panei et al. 2007; Steinfadt et al. 2010), and therefore it might be that the luminosity we see is dominated by gravitational contraction (but see Driebe et al. 1998). If that is true, then we estimate a thermal timescale of $2d_2^{-3}$ Myr for an effective temperature of 18,000 K considering the whole star—the timescale would be $2d_2^{-3}$ kyr if we only are concerned with a typical envelope of $10^{-3}\,M_\odot$ (Panei et al. 2007)—so if the companion is larger than a typical low-mass white dwarf, then it is likely extremely young, and we might be seeing a newly born millisecond pulsar slightly after the transitional phase found by Archibald et al. (2009). The hot/large state could also be a result of a recent hydrogen flash. This source then resembles the rather young WD/sdB stars HD 188112 ($T_{\rm eff}$ =21,500 K, $M = 0.24\,M_\odot$, $R = 0.1\,R_\odot$; Heber et al. 2003) or GALEX J1717+6757 ($T_{\rm eff}$ =14,900 K, $M = 0.19\,M_\odot$, $R = 0.1\,R_\odot$; Vennes et al. 2011), which are thought to be progenitors of more typical helium-core white dwarfs. Both of these scenarios (mass stripping or hydrogen flash) are possibilities for the hot, bloated white dwarfs seen by *Kepler* (van Kerkwijk et al. 2010; Carter et al. 2011; Breton et al. 2012), which the companion to PSR J1816+4510 also resembles, although the presence of a neutron star instead of a main sequence primary would require a different evolution. Again, spectroscopy to determine surface gravity and elemental abundances should be definitive. Finally, it is possible that, despite the eclipses the system is closer to face-on than edge on, as for inclinations of $<30^\circ$ the companion mass is $>0.5\,M_\odot$ like other hot white dwarf companions. This would be contrary to the theoretical companion mass versus orbital period relation (Tauris & Savonije 1999) and would make the radius even stranger, but there is at least one known outlier from the companion mass versus orbital period relation with a

substantially higher mass than expected (Hessels et al. 2005; Demorest et al. 2010).

The bright counterpart makes optical astrometry within the reach of ground-based telescopes, at least for determining a proper motion. While we see no definitive proper motion comparing the *Swift* and WIYN data (taken 0.6 yr apart), individual ground-based images can determine the relative position of the pulsar to $\lesssim$10 mas in only a few minutes. We expect a proper motion of $\mu = 10 v_{100} d_2^{-1}$ mas yr^{-1}, so assuming adequate calibration, this can be measured in a year or two. We could then compare this against any radio proper motion determined from timing, which would further establish whether or not the optical source is indeed the companion of the pulsar.

5. CONCLUSIONS

We have discovered the almost certain optical/UV counterpart of the newly discovered millisecond radio/γ-ray pulsar PSR J1816+4510. The radio/γ-ray properties of PSR J1816+4510 appear much like most energetic eclipsing pulsars discovered recently (Roberts 2011), which supports the use of *Fermi* and low-frequency radio observations to find energetic recycled pulsars. Some aspects of PSR J1816+4510's radio properties appear unique, in that the plausible size of the eclipsing region seems to be contained in its companion's Roche lobe, but such inferences depend on the inclination as well as the observing frequency of the radio data.

While we still cannot constrain all of its parameters uniquely, the optical/UV properties of PSR J1816+4510 appear more robustly unique, with an effective temperature likely at least three times higher than any other black-widow or redback system. In fact, the companion may be the brightest low-mass (i.e., not a B star) optical[27] companion to any pulsar (van Kerkwijk et al. 2005). This is largely because of the high temperature rather than a small distance or large size. The high temperature presents a number of puzzles and opportunities. Depending on the radius, it may be that the companion is rather young, and that we are seeing the sources only shortly after its envelope was stripped away. Phase-resolved photometry and spectroscopy will be important to determine the orientation and mass function of the system (van Kerkwijk et al. 2011), and radio astrometry can help constrain the radius of the companion. Long-term optical monitoring may be able to detect cooling after a recent stripping or burning episode. Given how bright it is, modulation of the companion may be detectable from a number of mechanisms. Orbital motion may be visible through Doppler boosting (van Kerkwijk et al. 2010; Shporer et al. 2010), which is expected to produce modulation of $\pm 0.3\%$, while ellipsoidal modulations ($\pm 0.1\%$) could help constrain the mass ratio and/or the degree of Roche lobe filling (van Kerkwijk et al. 2010; Carter et al. 2011; Breton et al. 2012). At the same time, the high temperature and small size compared to the Roche lobe mean that the photocenter may be much closer to the geometric center of the star (cf. van Kerkwijk et al. 2011) facilitating (along with its brightness) measurement and interpretation of the radial velocity curve, and with it enabling an accurate mass measurement for this neutron star.

We thank an anonymous referee for useful comments, P. Ray, L. Bildsten, S. Phinney, R. Breton, M. van Kerkwijk, and C. Bassa for helpful discussions, and D. Koester for supplying some white dwarf atmosphere models. Based upon data from the WIYN Observatory, which is a joint facility of the University of Wisconsin-Madison, Indiana University, Yale University and the National Optical Astronomy Observatories. The National Radio Astronomy Observatory is a facility of the National Science Foundation operated under cooperative agreement by Associated Universities, Inc. Some of the data presented in this paper were obtained from the Multimission Archive at the Space Telescope Science Institute (MAST). STScI is operated by the Association of Universities for Research in Astronomy, Inc., under NASA contract NAS5-26555. Support for MAST for non-HST data is provided by the NASA Office of Space Science via grant NNX09AF08G and by other grants and contracts. J.W.T.H. is a Veni Fellow of the Netherlands Foundation for Scientific Research (NWO). C.M.B., D.F.D., M.D.W.R., and X.S. were supported by NSF CAREER award number 09955929 and PIRE award number 0968126, with additional support from the University of Wisconsin–Milwaukee Office of Undergraduate Research. Pulsar research at UBC is supported by an NSERC Discovery Grant.

Facilities: Fermi (LAT), *Swift* (UVOT, XRT), *GALEX*, WIYN (MiniMo)

[27] It is expected to be as bright as the companion to PSR J0437−4715 in the near-infrared (Durant et al. 2011), consistent with its non-detection in 2MASS.

REFERENCES

Abdo, A. A., Ackermann, M., Ajello, M., et al. 2009, Science, 325, 848
Abdo, A. A., Ackermann, M., Ajello, M., et al. 2011, ApJ, 736, L11
Archibald, A. M., Stairs, I. H., Ransom, S. M., et al. 2009, Science, 324, 1411
Arons, J., & Tavani, M. 1993, ApJ, 403, 249
Atwood, W. B., Abdo, A. A., Ackermann, M., et al. 2009, ApJ, 697, 1071
Bassa, C. G., van Kerkwijk, M. H., Koester, D., & Verbunt, F. 2006, A&A, 456, 295
Bell, J. F., Bailes, M., Manchester, R. N., Weisberg, J. M., & Lyne, A. G. 1995, ApJ, 440, L81
Bertin, E., & Arnouts, S. 1996, A&AS, 117, 393
Bessell, M. S., Castelli, F., & Plez, B. 1998, A&A, 333, 231
Breton, R. P., Rappaport, S. A., van Kerkwijk, M. H., & Carter, J. A. 2012, ApJ, 748, 115
Brown, W. R., Kilic, M., Hermes, J. J., et al. 2011, ApJ, 737, L23
Burrows, D. N., Hill, J. E., Nousek, J. A., et al. 2005, Space Sci. Rev., 120, 165
Cardelli, J. A., Clayton, G. C., & Mathis, J. S. 1989, ApJ, 345, 245
Carter, J. A., Rappaport, S., & Fabrycky, D. 2011, ApJ, 728, 139
Chatterjee, S., Brisken, W. F., Vlemmings, W. H. T., et al. 2009, ApJ, 698, 250
Cocozza, G., Ferraro, F. R., Possenti, A., et al. 2008, ApJ, 679, L105
Cognard, I., Guillemot, L., Johnson, T. J., et al. 2011, ApJ, 732, 47
Cordes, J. M., & Lazio, T. J. W. 2002, arXiv:astro-ph/0207156
Cox, A. N. 2000, Allen's Astrophysical Quantities (4th ed.; New York: AIP/Springer)
D'Amico, N., Possenti, A., Manchester, R. N., et al. 2001, ApJ, 561, L89
de Jager, O. C., Raubenheimer, B. C., & Swanepoel, J. W. H. 1989, A&A, 221, 180
Demorest, P. B., Pennucci, T., Ransom, S. M., Roberts, M. S. E., & Hessels, J. W. T. 2010, Nature, 467, 1081
Drake, A. J., Djorgovski, S. G., Mahabal, A., et al. 2009, ApJ, 696, 870
Driebe, T., Schoenberner, D., Bloecker, T., & Herwig, F. 1998, A&A, 339, 123
Drimmel, R., Cabrera-Lavers, A., & López-Corredoira, M. 2003, A&A, 409, 205
Durant, M., Kargaltsev, O., Pavlov, G. G., et al. 2011, ApJ, 746, 6
Durant, M., & van Kerkwijk, M. H. 2006, ApJ, 650, 1070
Eggleton, P. P. 1983, ApJ, 268, 368
Ferraro, F. R., Possenti, A., D'Amico, N., & Sabbi, E. 2001, ApJ, 561, L93
Fontaine, G., Brassard, P., & Bergeron, P. 2001, PASP, 113, 409
Fruchter, A. S., Stinebring, D. R., & Taylor, J. H. 1988, Nature, 333, 237
Gaensler, B. M., Madsen, G. J., Chatterjee, S., & Mao, S. A. 2008, PASA, 25, 184
Hansen, B. M. S., & Liebert, J. 2003, ARA&A, 41, 465
Heber, U., Edelmann, H., Lisker, T., & Napiwotzki, R. 2003, A&A, 411, L477
Hessels, J., Ransom, S., Roberts, M., et al. 2005, in ASP Conf. Ser. 328, Binary Radio Pulsars, ed. F. A. Rasio & I. H. Stairs (San Francisco, CA: ASP), 395

Hessels, J. W. T., Roberts, M. S. E., McLaughlin, M. A., et al. 2011, in AIP Conf. Ser. 1357, Radio Pulsars: An Astrophysical Key to Unlock the Secrets of the Universe, ed. M. Burgay, N. D'Amico, P. Esposito, A. Pellizzoni, & A. Possenti (Melville, NY: AIP), 40
Hobbs, G. B., Edwards, R. T., & Manchester, R. N. 2006, MNRAS, 369, 655
Keith, M. J., Johnston, S., Ray, P. S., et al. 2011, MNRAS, 414, 1292
Kerr, M., Camilo, F., Johnson, T. J., et al. 2012, ApJ, 748, L2
Kotulla, R., Fritze, U., Weilbacher, P., & Anders, P. 2009, MNRAS, 396, 462
Kulkarni, S. R., & Hester, J. J. 1988, Nature, 335, 801
Kurucz, R. 1993, ATLAS9 Stellar Atmosphere Programs and 2 km/s Grid. Kurucz CD-ROM No. 13 (Cambridge, MA: Smithsonian Astrophysical Observatory)
Lorimer, D. R., Lyne, A. G., Festin, L., & Nicastro, L. 1995, Nature, 376, 393
Monet, D. G., Levine, S. E., Canzian, B., et al. 2003, AJ, 125, 984
Morrissey, P., Conrow, T., Barlow, T. A., et al. 2007, ApJS, 173, 682
Nice, D. J., & Taylor, J. H. 1995, ApJ, 441, 429
Nolan, P. L., Abdo, A. A., Ackerman, M., et al. 2012, ApJS, 199, 3
O'Donnell, J. E. 1994, ApJ, 422, 158
Paczynski, B. 1976, in IAU Symp. 73, Structure and Evolution of Close Binary Systems, ed. P. Eggleton, S. Mitton, & J. Whelan (Cambridge: Cambridge Univ. Press), 75
Pallanca, C., Dalessandro, E., Ferraro, F. R., et al. 2010, ApJ, 725, 1165
Panei, J. A., Althaus, L. G., Chen, X., & Han, Z. 2007, MNRAS, 382, 779
Phinney, E. S., Evans, C. R., Blandford, R. D., & Kulkarni, S. R. 1988, Nature, 333, 832
Possenti, A., Cerutti, R., Colpi, M., & Mereghetti, S. 2002, A&A, 387, 993
Predehl, P., & Schmitt, J. H. M. M. 1995, A&A, 293, 889
Ransom, S. M., Ray, P. S., Camilo, F., et al. 2011, ApJ, 727, L16
Reynolds, M. T., Callanan, P. J., Fruchter, A. S., et al. 2007, MNRAS, 379, 1117
Roberts, M. S. E. 2011, in AIP Conf. Ser. 1357, Radio Pulsars: An Astrophysical Key to Unlock the Secrets of the Universe, ed. M. Burgay, N. D'Amico, P. Esposito, A. Pellizzoni, & A. Possenti (Melville, NY: AIP), 127
Roming, P. W. A., Kennedy, T. E., Mason, K. O., et al. 2005, Space Sci. Rev., 120, 95
Saha, A., Armandroff, T., Sawyer, D. G., & Corson, C. 2000, Proc. SPIE, 4008, 447
Sarna, M. J., Ergma, E., & Gerškevitš-Antipova, J. 2000, MNRAS, 316, 84
Schlegel, D. J., Finkbeiner, D. P., & Davis, M. 1998, ApJ, 500, 525
Shakura, N. I., & Sunyaev, R. A. 1973, A&A, 24, 337
Shklovskii, I. S. 1970, SvA, 13, 562
Shporer, A., Kaplan, D. L., Steinfadt, J. D. R., et al. 2010, ApJ, 725, L200
Skrutskie, M. F., Cutri, R. M., Stiening, R., et al. 2006, AJ, 131, 1163
Stappers, B. W., Bailes, M., Lyne, A. G., et al. 1996, ApJ, 465, L119
Stappers, B. W., Bailes, M., Lyne, A. G., et al. 2001, MNRAS, 321, 576
Stappers, B. W., Gaensler, B. M., Kaspi, V. M., van der Klis, M., & Lewin, W. H. G. 2003, Science, 299, 1372
Steinfadt, J. D. R., Bildsten, L., & Arras, P. 2010, ApJ, 718, 441
Stetson, P. B. 2000, PASP, 112, 925
Takata, J., Cheng, K. S., & Taam, R. E. 2012, ApJ, 745, 100
Tauris, T. M., & Savonije, G. J. 1999, A&A, 350, 928
Unglaub, K. 2008, A&A, 486, 923
Unglaub, K., & Bues, I. 1998, A&A, 338, 75
van Kerkwijk, M. H., Bassa, C. G., Jacoby, B. A., & Jonker, P. G. 2005, in ASP Conf. Ser. 328, Binary Radio Pulsars, ed. F. A. Rasio & I. H. Stairs (San Francisco, CA: ASP), 357
van Kerkwijk, M. H., Breton, R. P., & Kulkarni, S. R. 2011, ApJ, 728, 95
van Kerkwijk, M. H., Rappaport, S. A., Breton, R. P., et al. 2010, ApJ, 715, 51
Vennes, S., Thorstensen, J. R., Kawka, A., et al. 2011, ApJ, 737, L16
Verbiest, J. P. W., Bailes, M., van Straten, W., et al. 2008, ApJ, 679, 675
Vink, J. S., & Cassisi, S. 2002, A&A, 392, 553
Vrtilek, S. D., Raymond, J. C., Garcia, M. R., et al. 1990, A&A, 235, 162
Webbink, R. F. 1975, MNRAS, 171, 555
Zavlin, V. E. 2007, Ap&SS, 308, 297